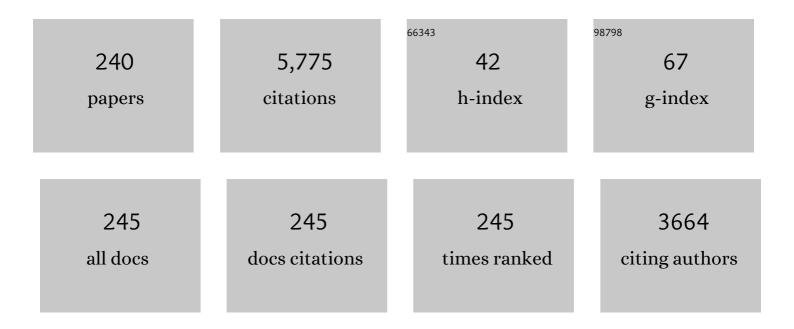
Timothy C Zhu

List of Publications by Year in descending order

Source: https://exaly.com/author-pdf/8542218/publications.pdf Version: 2024-02-01



| # | Article | IF | CITATIONS |
|----|---|-----|-----------|
| 1 | Validation of multispectral singlet oxygen luminescence dosimetry (MSOLD) for photofrin-mediated photodynamic therapy. , 2022, 11940, . | | 0 |
| 2 | Monte Carlo simulation of Cerenkov imaging for total skin electron treatment with CT DICOM realistic patient geometry. , 2022, 11940, . | | 0 |
| 3 | Reactive oxygen species explicit dosimetry (ROSED) for fractionated photofrin-mediated photodynamic therapy (PDT). , 2022, 11940, . | | 1 |
| 4 | Real-time PDT dose dosimetry for pleural photodynamic therapy. , 2022, 11940, . | | 5 |
| 5 | Determination of the distribution of drug concentration and tissue optical properties for ALA-mediated photodynamic therapy. , 2021, 11628, . | | 0 |
| 6 | A comparison of two probes to determine rectum optical properties. , 2021, 11628, . | | 0 |
| 7 | Monte Carlo (MC) study of dose distribution and Cherenkov imaging in total skin electron therapy (TSET) with TOPAS. , 2021, 11628, . | | 1 |
| 8 | Estimation of fluorescence probing depth dependence on the distance between source and detector using Monte Carlo modeling. , 2021, 11628, . | | 1 |
| 9 | Cherenkov imaging for total skin electron therapy: an evaluation of dose uniformity. , 2021, 11628, . | | 2 |
| 10 | Report of AAPM Task Group 219 on independent calculationâ€based dose/MU verification for IMRT. Medical Physics, 2021, 48, e808-e829. | 3.0 | 50 |
| 11 | Cherenkov imaging for total skin electron therapy (TSET). Medical Physics, 2020, 47, 201-212. | 3.0 | 22 |
| 12 | Evaluation of Light Fluence Distribution Using an IR Navigation System for HPPHâ€mediated Pleural Photodynamic Therapy (pPDT). Photochemistry and Photobiology, 2020, 96, 310-319. | 2.5 | 16 |
| 13 | Reactive Oxygen Species Explicit Dosimetry for Photofrinâ€mediated Pleural Photodynamic Therapy. Photochemistry and Photobiology, 2020, 96, 340-348. | 2.5 | 15 |
| 14 | ¹ O ₂ determined from the measured PDT dose and ³ O ₂ predicts long-term response to Photofrin-mediated PDT. Physics in Medicine and Biology, 2020, 65, 03LT01. | 3.0 | 6 |
| 15 | In Memoriam Jarod C. Finlay, PhD. Photochemistry and Photobiology, 2020, 96, 218-218. | 2.5 | 0 |
| 16 | In vivo Spectroscopic Evaluation of the Intraperitoneal Cavity in Canines. Photochemistry and Photobiology, 2020, 96, 426-433. | 2.5 | 3 |
| 17 | Blood Flow Measurements Enable Optimization of Light Delivery for Personalized Photodynamic Therapy. Cancers, 2020, 12, 1584. | 3.7 | 8 |
| 18 | Infrared navigation system for light dosimetry during pleural photodynamic therapy. Physics in Medicine and Biology, 2020, 65, 075006. | 3.0 | 16 |

| # | Article | IF | CITATIONS |
|----|---|-----|-----------|
| 19 | Light Fluence Rate and Tissue Oxygenation (S _t O ₂) Distributions Within the Thoracic Cavity of Patients Receiving Intraoperative Photodynamic Therapy for Malignant Pleural Mesothelioma. Photochemistry and Photobiology, 2020, 96, 417-425. | 2.5 | 5 |
| 20 | Reactive oxygen species explicit dosimetry to predict tumor growth for benzoporphyrin derivative-mediated vascular photodynamic therapy. Journal of Biomedical Optics, 2020, 25, 1. | 2.6 | 6 |
| 21 | Reactive oxygen species explicit dosimetry to predict local tumor growth for Photofrin-mediated photodynamic therapy. Biomedical Optics Express, 2020, 11, 4586. | 2.9 | 10 |
| 22 | Special Section Guest Editorial: Photodynamic Therapy. Journal of Biomedical Optics, 2020, 25, 1. | 2.6 | 0 |
| 23 | Computer animation body surface analysis of total skin electron radiation therapy dose homogeneity via Cherenkov imaging. Journal of Medical Imaging, 2020, 7, 1. | 1.5 | 4 |
| 24 | Cherenkov imaging of total skin electron irradiation (TSEI). Journal of Physics: Conference Series, 2019, 1305, 012016. | 0.4 | 1 |
| 25 | Reactive oxygen species explicit dosimetry to predict local tumor control for Photofrin-mediated photodynamic therapy. , 2019, 10860, . | | 6 |
| 26 | Important Technical Considerations for Implementing the ASTRO/ASCO/AUA Prostate Cancer Hypofractionated Radiation Guideline. Practical Radiation Oncology, 2019, 9, 197-199. | 2.1 | 2 |
| 27 | A Novel Prospective Study Assessing the Combination of Photodynamic Therapy and Proton Radiation Therapy: Safety and Outcomes When Treating Malignant Pleural Mesothelioma. Photochemistry and Photobiology, 2019, 95, 411-418. | 2.5 | 19 |
| 28 | Validation of combined Monte Carlo and photokinetic simulations for the outcome correlation analysis of benzoporphyrin derivative-mediated photodynamic therapy on mice. Journal of Biomedical Optics, 2019, 24, 1. | 2.6 | 11 |
| 29 | Validation of tissue optical properties measurement using diffuse reflectance spectroscopy (DRS). , 2019, 10860, . | | 5 |
| 30 | Analysis of cumulative surface dose based on Cherenkov imaging of Total Skin Electron Therapy (TSET). , 2019, , . | | 0 |
| 31 | Monte Carlo investigation of the effect of skin tissue optical properties on detected Cherenkov emission. , 2019, 10862, . | | 2 |
| 32 | Reactive oxygen species explicit dosimetry to predict tumor growth for BPD-mediated vascular photodynamic therapy. , 2019, 10861, . | | 0 |
| 33 | Determination of in-vivo tissue optical properties for anal photodynamic therapy. , 2019, , . | | 0 |
| 34 | Image guidance doses delivered during radiotherapy: Quantification, management, and reduction: Report of the <scp>AAPM</scp> Therapy Physics Committee Task Group 180. Medical Physics, 2018, 45, e84-e99. | 3.0 | 104 |
| 35 | Fluorescenceâ€guided surgery and intervention — An <scp>AAPM</scp> emerging technology blue paper. Medical Physics, 2018, 45, 2681-2688. | 3.0 | 29 |
| 36 | Lesion oxygenation associates with clinical outcomes in premalignant and early stage head and neck tumors treated on a phase 1 trial of photodynamic therapy. Photodiagnosis and Photodynamic Therapy, 2018, 21, 28-35. | 2.6 | 30 |

| # | Article | IF | CITATIONS |
|----|---|-----|-----------|
| 37 | PDT dose dosimetry for Photofrin-mediated pleural photodynamic therapy (pPDT). Physics in Medicine and Biology, 2018, 63, 015031. | 3.0 | 31 |
| 38 | A quality assurance program for clinical PDT. , 2018, 10476, . | | 1 |
| 39 | Reactive oxygen species explicit dosimetry (ROSED) of a type 1 photosensitizer. , 2018, 10476, . | | 2 |
| 40 | Monte Carlo modeling of fluorescence in semi-infinite turbid media. , 2018, 10492, . | | 2 |
| 41 | Cherenkov imaging for Total Skin Electron Therapy (TSET). , 2018, , . | | 5 |
| 42 | Light fluence dosimetry in lung-simulating cavities. , 2018, 10476, . | | 1 |
| 43 | Determination of optical properties, drug concentration, and tissue oxygenation in human pleural tissue before and after Photofrin-mediated photodynamic therapy. , 2018, 10476, . | | 0 |
| 44 | A Comparison of Dose Metrics to Predict Local Tumor Control for Photofrinâ€mediated Photodynamic Therapy. Photochemistry and Photobiology, 2017, 93, 1115-1122. | 2.5 | 22 |
| 45 | Evaluation of singlet oxygen explicit dosimetry for predicting treatment outcomes of benzoporphyrin derivative monoacid ring A-mediated photodynamic therapy. Journal of Biomedical Optics, 2017, 22, 028002. | 2.6 | 25 |
| 46 | On the <i>in vivo</i> photochemical rate parameters for PDT reactive oxygen species modeling. Physics in Medicine and Biology, 2017, 62, R1-R48. | 3.0 | 68 |
| 47 | Four-channel PDT dose dosimetry for pleural photodynamic therapy. , 2017, , . | | 2 |
| 48 | Singlet oxygen explicit dosimetry to predict long-term local tumor control for Photofrin-mediated photodynamic therapy. Proceedings of SPIE, 2017, , . | 0.8 | 1 |
| 49 | Three-dimensional finite-element based deformable image registration for evaluation of pleural cavity irradiation during photodynamic therapy. Medical Physics, 2017, 44, 3767-3775. | 3.0 | 1 |
| 50 | Singlet oxygen explicit dosimetry to predict long-term local tumor control for BPD-mediated photodynamic therapy. Proceedings of SPIE, 2017, , . | 0.8 | 2 |
| 51 | Oxygen measurements to improve singlet oxygen dosimetry. , 2017, , . | | 0 |
| 52 | Patterns of Dose Prescription and Recording inÂStereotactic Body Radiation Therapy: AÂMulti-institutional Study. International Journal of Radiation Oncology Biology Physics, 2017, 99, S68-S69. | 0.8 | 0 |
| 53 | 31 P NMR Evidence for Peroxide Intermediates in Lipid Emulsion Photooxidations: Phosphine Substituent Effects in Trapping. Photochemistry and Photobiology, 2017, 93, 1430-1438. | 2.5 | 3 |
| 54 | A summary of light dose distribution using an IR navigation system for Photofrin-mediated Pleural PDT. Proceedings of SPIE, 2017, 10047, . | 0.8 | 6 |

| # | Article | IF | CITATIONS |
|----|--|------------------|-----------|
| 55 | State of dose prescription and compliance to international standard (ICRU-83) in intensity modulated radiation therapy among academic institutions. Practical Radiation Oncology, 2017, 7, e145-e155. | 2.1 | 38 |
| 56 | A compact fiberâ€optic probeâ€based singlet oxygen luminescence detection system. Journal of Biophotonics, 2017, 10, 320-326. | 2.3 | 22 |
| 57 | Monitoring and assessment of tumor hemodynamics during pleural PDT. Proceedings of SPIE, 2017, , . | 0.8 | 1 |
| 58 | 21 Spectroscopic imaging in prostate PDT. Series in Cellular and Clinical Imaging, 2017, , 419-454. | 0.2 | 0 |
| 59 | Singlet oxygen explicit dosimetry to predict local tumor control for HPPH-mediated photodynamic therapy. Proceedings of SPIE, 2017, , . | 0.8 | 1 |
| 60 | A Comparison of Singlet Oxygen Explicit Dosimetry (SOED) and Singlet Oxygen Luminescence Dosimetry (SOLD) for Photofrin-Mediated Photodynamic Therapy. Cancers, 2016, 8, 109. | 3.7 | 23 |
| 61 | Analytic function for predicting light fluence rate of circular fields on a semi-infinite turbid medium. Optics Express, 2016, 24, 26261. | 3.4 | 25 |
| 62 | Evaluation of the 2â€(1â€Hexyloxyethyl)â€2â€devinyl pyropheophorbide (HPPH) mediated photodynamic therapy by macroscopic singlet oxygen modeling. Journal of Biophotonics, 2016, 9, 1344-1354. | [/] 2.3 | 24 |
| 63 | Proton computed tomography using a 1D silicon diode array. Medical Physics, 2016, 43, 5758-5766. | 3.0 | 3 |
| 64 | Explicit macroscopic singlet oxygen modeling for benzoporphyrin derivative monoacid ring A (BPD)-mediated photodynamic therapy. Journal of Photochemistry and Photobiology B: Biology, 2016, 164, 314-322. | 3.8 | 17 |
| 65 | Macroscopic singlet oxygen modeling for dosimetry of Photofrin-mediated photodynamic therapy: an <i>in-vivo</i> study. Journal of Biomedical Optics, 2016, 21, 088002. | 2.6 | 41 |
| 66 | PDT dose dosimeter for pleural photodynamic therapy. Proceedings of SPIE, 2016, 9694, 96940Y. | 0.8 | 15 |
| 67 | Determination of the low concentration correction in the macroscopic singlet oxygen model for PDT. , 2016, 9694, 96940D. | | 1 |
| 68 | Investigating the impact of oxygen concentration and blood flow variation on photodynamic therapy. Proceedings of SPIE, 2016, 9694, . | 0.8 | 8 |
| 69 | Dosimetry study of PHOTOFRIN-mediated photodynamic therapy in a mouse tumor model. Proceedings of SPIE, 2016, 9694, . | 0.8 | 10 |
| 70 | An improved analytic function for predicting light fluence rate in circular fields on a semi-infinite geometry. Proceedings of SPIE, 2016, 9706, 97061D. | 0.8 | 5 |
| 71 | A feasibility study of singlet oxygen explicit dosmietry (SOED) of PDT by intercomparison with a singlet oxygen luminescence dosimetry (SOLD) system. , 2016, 9694, . | | 4 |
| 72 | Toxicities and early outcomes in a phase 1 trial of photodynamic therapy for premalignant and early stage head and neck tumors. Oral Oncology, 2016, 55, 37-42. | 1.5 | 27 |

| # | Article | IF | CITATIONS |
|----|---|-----|-----------|
| 73 | Deformable medical image registration of pleural cavity for photodynamic therapy by using finite-element based method. , 2016, 9701, 970106. | | 3 |
| 74 | Fiber optic probes based on silver-only coated hollow glass waveguides for ionizing beam radiation dosimetry. Proceedings of SPIE, 2016, , . | 0.8 | 4 |
| 75 | Measuring the Physiologic Properties of Oral Lesions Receiving Fractionated Photodynamic Therapy. Photochemistry and Photobiology, 2015, 91, 1210-1218. | 2.5 | 18 |
| 76 | An IR navigation system for pleural PDT. Frontiers in Physics, 2015, 3, . | 2.1 | 18 |
| 77 | Study of tissue oxygen supply rate in a macroscopic photodynamic therapy singlet oxygen model. Journal of Biomedical Optics, 2015, 20, 038001. | 2.6 | 44 |
| 78 | Parameterization of electron beam output factor. Physica Medica, 2015, 31, 420-424. | 0.7 | 4 |
| 79 | In-vivo singlet oxygen threshold doses for PDT. Photonics & Lasers in Medicine, 2015, 4, 59-71. | 0.2 | 44 |
| 80 | In-vivo outcome study of HPPH mediated PDT using singlet oxygen explicit dosimetry (SOED). , 2015, 9308, . | | 9 |
| 81 | <i>In vivo</i> outcome study of BPD-mediated PDT using a macroscopic singlet oxygen model. Proceedings of SPIE, 2015, 9308, . | 0.8 | 12 |
| 82 | Real-time treatment light dose guidance of Pleural PDT: an update. Proceedings of SPIE, 2015, 9308, . | 0.8 | 9 |
| 83 | Dose Prescription and Recording Variability in the Era of ICRU-83: A Multi-institutional Study. International Journal of Radiation Oncology Biology Physics, 2015, 93, S42-S43. | 0.8 | 0 |
| 84 | Macroscopic singlet oxygen model incorporating photobleaching as an input parameter. , 2015, 9308, 93080V. | | 5 |
| 85 | Explicit dosimetry for 2-(1-hexyloxyethyl)-2-devinyl pyropheophorbide-a-mediated photodynamic therapy: macroscopic singlet oxygen modeling. Journal of Biomedical Optics, 2015, 20, 128003. | 2.6 | 38 |
| 86 | Phosphor-based fiber optic microprobes for ionizing beam radiation dosimetry. Proceedings of SPIE, 2015, , . | 0.8 | 6 |
| 87 | Clinical decision tool for optimal delivery of liver stereotactic body radiation therapy: Photons versus protons. Practical Radiation Oncology, 2015, 5, 209-218. | 2.1 | 53 |
| 88 | TIMP1 in conditioned media of human adipose stromal cells protects neurons against oxygen-glucose deprivation injury. Neuroscience Letters, 2015, 584, 56-59. | 2.1 | 10 |
| 89 | Diffuse optical tomography using multichannel robotic platform for interstitial PDT. Proceedings of SPIE, 2014, 8931, . | 0.8 | 0 |
| 90 | Comparison of singlet oxygen threshold dose for PDT. Proceedings of SPIE, 2014, 8931, . | 0.8 | 19 |

| # | Article | IF | CITATIONS |
|-----|--|-----|-----------|
| 91 | Anisotropic modeling for IR navigation-based PDT dosimetry. , 2014, 8931, . | | 1 |
| 92 | Determination of tissue optical properties in PDT treated head and neck patients. Proceedings of SPIE, 2014, 8926, . | 0.8 | 6 |
| 93 | Parameter determination for BPD mediated vascularPDT. Proceedings of SPIE, 2014, 8931, . | 0.8 | 5 |
| 94 | Bengt E. BjÄ ¤ ngard, Ph.D Medical Physics, 2014, 41, 040801. | 3.0 | 0 |
| 95 | Comparison of PDT parameters for RIF and H460 tumor models during HPPH-mediated PDT. Proceedings of SPIE, 2014, 8931, . | 0.8 | 12 |
| 96 | Development and validation of a treatment decision model for optimal delivery of liver stereotactic body radiation therapy (SBRT): Photons versus protons Journal of Clinical Oncology, 2014, 32, 264-264. | 1.6 | 0 |
| 97 | SU-E-T-577: Commissioning of a Deterministic Algorithm for External Photon Beams. Medical Physics, 2014, 41, 360-360. | 3.0 | 0 |
| 98 | SU-D-16A-07: Photobleaching Predicts Necrosis in Interstitial PDT. Medical Physics, 2014, 41, 109-109. | 3.0 | 0 |
| 99 | Should image rotation be addressed during routine cone-beam CT quality assurance?. Physics in Medicine and Biology, 2013, 58, 1059-1073. | 3.0 | 3 |
| 100 | A novel near real-time laser scanning device for geometrical determination of pleural cavity surface. , 2013, 8568, . | | 0 |
| 101 | A robotic multi-channel platform for interstitial photodynamic therapy. Proceedings of SPIE, 2013, 8568, 85680Q. | 0.8 | 2 |
| 102 | Monte Carlo simulation of light fluence calculation during pleural PDT. , 2013, 8568, . | | 3 |
| 103 | PDT dose dosimetry for pleural photodynamic therapy. Proceedings of SPIE, 2013, 8568, . | 0.8 | 12 |
| 104 | Parameter determination for singlet oxygen modeling of BPD-mediated PDT. Proceedings of SPIE, 2013, 8568, . | 0.8 | 11 |
| 105 | Real-time treatment feedback guidance of Pleural PDT. , 2013, 8568, . | | 8 |
| 106 | A theoretical and experimental examination of fluorescence in enclosed cavities. Proceedings of SPIE, 2013, 8568, . | 0.8 | 3 |
| 107 | Light dosimetry and dose verification for pleural PDT. Proceedings of SPIE, 2013, 8568, . | 0.8 | 0 |
| 108 | A theoretical comparison of macroscopic and microscopic modeling of singlet oxygen during Photofrin and HPPH mediated-PDT. Proceedings of SPIE, 2013, 8568, . | 0.8 | 6 |

| # | Article | IF | CITATIONS |
|-----|--|-----|-----------|
| 109 | Feasibility of interstitial diffuse optical tomography using cylindrical diffusing fibers for prostate PDT. Physics in Medicine and Biology, 2013, 58, 3461-3480. | 3.0 | 14 |
| 110 | Absolute calibration of optical power for PDT: Report of AAPM TG140. Medical Physics, 2013, 40, 081501. | 3.0 | 7 |
| 111 | Determination of optical properties in heterogeneous turbid media using a cylindrical diffusing fiber. Physics in Medicine and Biology, 2012, 57, 6025-6046. | 3.0 | 15 |
| 112 | Characterization of tissue optical properties for prostate PDT using interstitial diffuse optical tomography. , 2012, 8210, . | | 4 |
| 113 | Light dose verification for pleural PDT. , 2012, 8210, . | | 1 |
| 114 | A real-time treatment guidance system for pleural PDT. Proceedings of SPIE, 2012, 8210, . | 0.8 | 5 |
| 115 | Maximizing fluence rate and field uniformity of light blanket for intraoperative PDT. Proceedings of SPIE, 2012, 8210, . | 0.8 | 4 |
| 116 | Direct and Inverse Solutions for Thermal- and Stress-Transients and the Analytical Determination of Boundary Conditions Using Remote Temperature or Strain Data. Journal of Pressure Vessel Technology, Transactions of the ASME, 2012, 134, . | 0.6 | 0 |
| 117 | Singlet oxygen dosimetry modeling for photodynamic therapy. Proceedings of SPIE, 2012, 8210, . | 0.8 | 13 |
| 118 | Dosimetry in Pleural Photodynamic Therapy. Journal of the National Comprehensive Cancer Network: JNCCN, 2012, 10, S-60-S-64. | 4.9 | 8 |
| 119 | Oxidative Stress and Photodynamic Therapy for Prostate Cancer. , 2012, , 277-300. | | 0 |
| 120 | Verification of monitor unit calculations for nonâ€IMRT clinical radiotherapy: Report of AAPM Task Group 114. Medical Physics, 2011, 38, 504-530. | 3.0 | 88 |
| 121 | Transoral robotic photodynamic therapy for the oropharynx. Photodiagnosis and Photodynamic Therapy, 2011, 8, 64-67. | 2.6 | 15 |
| 122 | Photodynamic therapy in the management of pre-malignant head and neck mucosal dysplasia and microinvasive carcinoma. Photodiagnosis and Photodynamic Therapy, 2011, 8, 75-85. | 2.6 | 29 |
| 123 | A study of light fluence rate distribution for PDT using MC simulation. , 2011, , . | | 1 |
| 124 | Determining how uncertainties in optical properties affect light dose calculations for PDT. , 2011, , . | | 0 |
| 125 | PDT is better than alternative therapies such as brachytherapy, electron beams, or lowâ€energy x rays for the treatment of skin cancers. Medical Physics, 2011, 38, 1133-1135. | 3.0 | 5 |
| 126 | A review of <i>inâ€vivo</i> optical properties of human tissues and its impact on PDT. Journal of Biophotonics, 2011, 4, 773-787. | 2.3 | 261 |

| # | Article | IF | CITATIONS |
|-----|--|-----|-----------|
| 127 | An IR navigation system for real-time treatment guidance of pleural PDT. Proceedings of SPIE, 2011, 7886, . | 0.8 | 11 |
| 128 | Backscatter correction factor for megavoltage photon beam. Medical Physics, 2011, 38, 5563-5568. | 3.0 | 5 |
| 129 | SU-E-T-218: In Vivo 3D Dose Verification for IMRT Using Electronic Portal Imaging Device (EPID). Medical Physics, 2011, 38, 3536-3536. | 3.0 | 0 |
| 130 | Monte Carlo simulation of the effect of miniphantom on inâ€ e ir output ratio. Medical Physics, 2010, 37, 5228-5237. | 3.0 | 3 |
| 131 | Explicit dosimetry for photodynamic therapy: macroscopic singlet oxygen modeling. Journal of Biophotonics, 2010, 3, 304-318. | 2.3 | 111 |
| 132 | Dosimetric Evaluation of a Volume Segmentation Algorithm for MRI-based Treatment Planning for Head and Neck Cancer. International Journal of Radiation Oncology Biology Physics, 2010, 78, S70. | 0.8 | 3 |
| 133 | Small Field: dosimetry in electron disequilibrium region. Journal of Physics: Conference Series, 2010, 250, 012056. | 0.4 | 6 |
| 134 | Modeling scatter-to-primary dose ratio for megavoltage photon beams. Medical Physics, 2010, 37, 5270-5278. | 3.0 | 9 |
| 135 | Pre-clinic study of uniformity of light blanket for intraoperative photodynamic therapy. , 2010, 7551, . | | 7 |
| 136 | A fast heterogeneous algorithm for light fluence rate for prostate photodynamic therapy. Proceedings of SPIE, 2010, 7551, . | 0.8 | 2 |
| 137 | In vivo light dosimetry for HPPH-mediated pleural PDT. Proceedings of SPIE, 2010, 7551, . | 0.8 | 9 |
| 138 | Spectroscopic evaluation of photodynamic therapy of the intraperitoneal cavity. , 2010, 7551, . | | 1 |
| 139 | A heterogeneous optimization algorithm for reacted singlet oxygen for interstitial PDT. , 2010, 7551, . | | 2 |
| 140 | A treatment planning system for pleural PDT. Proceedings of SPIE, 2010, 7551, . | 0.8 | 5 |
| 141 | Targeted laryngeal photodynamic therapy with a balloon diffusing light source. Photodiagnosis and Photodynamic Therapy, 2010, 7, 158-161. | 2.6 | 13 |
| 142 | Interference with the Jaffé method for creatinine following 5-aminolevulinic acid administration. Photodiagnosis and Photodynamic Therapy, 2010, 7, 268-274. | 2.6 | 7 |
| 143 | Reconstruction of optical properties using a diffusion model for interstitial diffuse optical tomography. Proceedings of SPIE, 2009, 7164, 71640P. | 0.8 | 2 |
| 144 | Reconstruction of hemodynamics and sensitizer distributions during interstitial PDT using spectroscopy with linear light sources. Proceedings of SPIE, 2009, 7380, . | 0.8 | 1 |

| # | Article | IF | CITATIONS |
|-----|---|-----|-----------|
| 145 | The design of a robotic multichannel platform for photodynamic therapy. Proceedings of SPIE, 2009, 7380, 738049. | 0.8 | 3 |
| 146 | Optimization of physiological parameter for macroscopic modeling of reacted singlet oxygen concentration in an in-vivo model. Proceedings of SPIE, 2009, 7164, 716400. | 0.8 | 9 |
| 147 | In vivo light dosimetry for pleural PDT. , 2009, 7164, . | | 16 |
| 148 | A light blanket for intraoperative photodynamic therapy. Proceedings of SPIE, 2009, 7380, 73801W. | 0.8 | 13 |
| 149 | A heterogeneous algorithm for PDT dose optimization for prostate. , 2009, 7164, 71640B. | | 3 |
| 150 | Dosimetric Implications of Pancreatic Tumor Motion when Treating with Intensity Modulated Radiation Therapy (IMRT). International Journal of Radiation Oncology Biology Physics, 2009, 75, S668-S669. | 0.8 | 0 |
| 151 | Reconstruction of in-vivo optical properties for human prostate using interstitial diffuse optical tomography. Optics Express, 2009, 17, 11665. | 3.4 | 36 |
| 152 | Fluence rate-dependent intratumor heterogeneity in physiologic and cytotoxic responses to Photofrin photodynamic therapy. Photochemical and Photobiological Sciences, 2009, 8, 1683-1693. | 2.9 | 59 |
| 153 | Diffuse reflectance spectra measured in vivo in human tissues during Photofrin-mediated pleural photodynamic therapy: updated results. Proceedings of SPIE, 2009, , . | 0.8 | 1 |
| 154 | Determination of correction factors for a 2D diode array device in MV photon beams. Medical Physics, 2009, 36, 523-529. | 3.0 | 6 |
| 155 | Report of AAPM Therapy Physics Committee Task Group 74: Inâ€air output ratio, , for megavoltage photon beams. Medical Physics, 2009, 36, 5261-5291. | 3.0 | 77 |
| 156 | Accelerator beam data commissioning equipment and procedures: Report of the TGâ€106 of the Therapy Physics Committee of the AAPM. Medical Physics, 2008, 35, 4186-4215. | 3.0 | 370 |
| 157 | Integrated light dosimetry system for prostate photodynamic therapy. Proceedings of SPIE, 2008, 6845, | 0.8 | 3 |
| 158 | Sensitivity analysis of imaging geometries for prostate diffuse optical tomography. Proceedings of SPIE, 2008, 6845, . | 0.8 | 2 |
| 159 | Interstitial diffuse optical tomography using an adjoint model with linear sources. , 2008, 6845, . | | 5 |
| 160 | Optimization of light source parameters in the photodynamic therapy of heterogeneous prostate. Physics in Medicine and Biology, 2008, 53, 4107-4121. | 3.0 | 27 |
| 161 | Motexafin Lutetium-Photodynamic Therapy of Prostate Cancer: Short- and Long-Term Effects on Prostate-Specific Antigen. Clinical Cancer Research, 2008, 14, 4869-4876. | 7.0 | 109 |
| 162 | Determination of <i>in vivo</i> light fluence distribution in a heterogeneous prostate during photodynamic therapy. Physics in Medicine and Biology, 2008, 53, 2103-2114. | 3.0 | 39 |

| # | Article | IF | CITATIONS |
|-----|---|-----|-----------|
| 163 | The role of photodynamic therapy (PDT) physics. Medical Physics, 2008, 35, 3127-3136. | 3.0 | 179 |
| 164 | Patient-Specific Dosimetry for Photodynamic Therapy. Lecture Notes in Electrical Engineering, 2008, , 115-125. | 0.4 | 0 |
| 165 | A method to improve reconstruction of the distribution of hemoglobin, oxygenation, and MLu concentration in the human prostate before and after photodynamic therapy. , 2007, 6427, 64270K. | | 0 |
| 166 | Two-dimensional/three-dimensional hybrid interstitial diffuse optical tomography of human prostate during photodynamic therapy: phantom and clinical results. , 2007, 6434, . | | 2 |
| 167 | Macroscopic modeling of the singlet oxygen production during PDT. , 2007, 6427, 642708. | | 37 |
| 168 | Quantitative comparison of tissue oxygen and motexafin lutetium uptake by ex vivo and noninvasive in vivo techniques in patients with intraperitoneal carcinomatosis. Journal of Biomedical Optics, 2007, 12, 034023. | 2.6 | 15 |
| 169 | Energy dependence of commercially available diode detectors forin-vivodosimetry. Medical Physics, 2007, 34, 1704-1711. | 3.0 | 49 |
| 170 | Modeling light fluence rate distribution in optically heterogeneous prostate photodynamic therapy using a kernel method. , 2007, 6427, . | | 2 |
| 171 | SUâ€FFâ€Tâ€12: A Fluenceâ€Based Algorithm for MU Calculation of Proton Beams. Medical Physics, 2007, 34, 2403-2403. | 3.0 | 0 |
| 172 | Prostate PDT dosimetry. Photodiagnosis and Photodynamic Therapy, 2006, 3, 234-246. | 2.6 | 52 |
| 173 | Photodynamic Therapy with Motexafin Lutetium for Rectal Cancer: A Preclinical Model in the Dog. Journal of Surgical Research, 2006, 135, 323-330. | 1.6 | 21 |
| 174 | Interstitial Fluorescence Spectroscopy in the Human Prostate During Motexafin Lutetium–Mediated Photodynamic Therapy. Photochemistry and Photobiology, 2006, 82, 1270. | 2.5 | 64 |
| 175 | Real-time In Situ Monitoring of Human Prostate Photodynamic Therapy with Diffuse Light. Photochemistry and Photobiology, 2006, 82, 1279. | 2.5 | 102 |
| 176 | Preliminary results of interstitial motexafin lutetium-mediated PDT for prostate cancer. Lasers in Surgery and Medicine, 2006, 38, 427-434. | 2.1 | 100 |
| 177 | Study of light fluence rate distribution in photodynamic therapy using finite-element method. , 2006, 6139, 127. | | 10 |
| 178 | In-vivo light dosimetry of interstitial PDT of human prostate. , 2006, 6139, 116. | | 7 |
| 179 | Measurement of in-air output ratios using different miniphantom materials. Physics in Medicine and Biology, 2006, 51, 3819-3834. | 3.0 | 9 |
| 180 | A Phase II Trial of Intraperitoneal Photodynamic Therapy for Patients with Peritoneal Carcinomatosis and Sarcomatosis. Clinical Cancer Research, 2006, 12, 2517-2525. | 7.0 | 102 |

| # | Article | IF | CITATIONS |
|-----|---|-----|-----------|
| 181 | Diffuse reflectance spectra measured in vivo in human tissues during Photofrin-mediated pleural photodynamic therapy. , 2006, 6139, . | | 15 |
| 182 | A macro-Monte Carlo method for the simulation of diffuse light transport in tissue. , 2006, 6139, . | | 1 |
| 183 | Updated Results of a Phase I Trial of Motexafin Lutetium-Mediated Interstitial Photodynamic Therapy in Patients with Locally Recurrent Prostate Cancer. Journal of Environmental Pathology, Toxicology and Oncology, 2006, 25, 373-388. | 1.2 | 78 |
| 184 | Detector calibration factor for interstitial in vivo light dosimetry using isotropic detectors with scattering tip. , 2005, 5689, . | | 9 |
| 185 | Determination of the distribution of light, optical properties, drug concentration, and tissue oxygenation in-vivo in human prostate during motexafin lutetium-mediated photodynamic therapy. Journal of Photochemistry and Photobiology B: Biology, 2005, 79, 231-241. | 3.8 | 187 |
| 186 | A method for determination of the absorption and scattering properties interstitially in turbid media. Physics in Medicine and Biology, 2005, 50, 2291-2311. | 3.0 | 94 |
| 187 | Optical Properties of Human Prostate at 732 nm Measured In Vivo During Motexafin Lutetium–mediated Photodynamic Therapy¶. Photochemistry and Photobiology, 2005, 81, 96. | 2.5 | 67 |
| 188 | Optimized interstitial PDT prostate treatment planning with the Cimmino feasibility algorithm. Medical Physics, 2005, 32, 3524-3536. | 3.0 | 57 |
| 189 | Optimization of light sources for prostate photodynamic therapy. , 2005, 5689, 186-197. | | 3 |
| 190 | In vivo measurement of fluorescence emission in the human prostate during photodynamic therapy. , 2005, 5689, 299-310. | | 3 |
| 191 | Broadband reflectance measurements of light penetration, blood oxygenation, hemoglobin concentration, and drug concentration in human intraperitoneal tissues before and after photodynamic therapy. Journal of Biomedical Optics, 2005, 10, 014004. | 2.6 | 101 |
| 192 | Optical Properties of Human Prostate at 732 nm Measured <i>In Vivo</i> During Motexafin Lutetium–mediated Photodynamic Therapy [¶] . Photochemistry and Photobiology, 2005, 81, 96-105. | 2.5 | 1 |
| 193 | Optical Properties of Human Prostate at 732 nm Measured In Vivo during Motexafin Lutetium-Mediated Photodynamic Therapy. Photochemistry and Photobiology, 2004, 81, 96-105. | 2.5 | 45 |
| 194 | Thermal and temporal response of ionization chambers in radiation dosimetry. Medical Physics, 2004, 31, 573-578. | 3.0 | 16 |
| 195 | Output ratio in air for MLC shaped irregular fields. Medical Physics, 2004, 31, 2480-2490. | 3.0 | 17 |
| 196 | Dose rate and SDD dependence of commercially available diode detectors. Medical Physics, 2004, 31, 914-924. | 3.0 | 67 |
| 197 | In vivo determination of the absorption and scattering spectra of the human prostate during photodynamic therapy. , 2004, 5315, 132-142. | | 21 |
| 198 | Phase II Trial of Pleural Photodynamic Therapy and Surgery for Patients With Non–Small-Cell Lung Cancer With Pleural Spread. Journal of Clinical Oncology, 2004, 22, 2192-2201. | 1.6 | 105 |

| # | Article | IF | CITATIONS |
|-----|---|-----|-----------|
| 199 | Light dosimetry at tissue surfaces for oblique incident circular fields. , 2004, 5315, 113-124. | | 8 |
| 200 | Phase I trial of motexafin-lutetium-mediated interstitial photodynamic therapy in patients with locally recurrent prostate cancer. , 2004, , . | | 19 |
| 201 | A phase I study of Foscan-mediated photodynamic therapy and surgery in patients with mesothelioma. Annals of Thoracic Surgery, 2003, 75, 952-959. | 1.3 | 125 |
| 202 | Head scatter off-axis for megavoltage x rays. Medical Physics, 2003, 30, 533-543. | 3.0 | 19 |
| 203 | Modeling the instantaneous dose rate dependence of radiation diode detectors. Medical Physics, 2003, 30, 2509-2519. | 3.0 | 58 |
| 204 | Light dosimetry at tissue surfaces for small circular fields. , 2003, 4952, 56-67. | | 11 |
| 205 | In-vivo measurements of penetration depth, oxygenation, and drug concentration using broadband absorption spectroscopy in human tissues before and after photodynamic therapy. , 2003, 4952, 68. | | 3 |
| 206 | In vivo Optical Properties of Normal Canine Prostate at 732 nm Using Motexafin Lutetium–mediated Photodynamic Therapy¶. Photochemistry and Photobiology, 2003, 77, 81. | 2.5 | 51 |
| 207 | In vivo Optical Properties of Normal Canine Prostate at 732 nm Using Motexafin Lutetium-mediated Photodynamic Therapy¶. Photochemistry and Photobiology, 2003, 77, 81-88. | 2.5 | 2 |
| 208 | <title>Ratio of the spherical and flat detectors at tissue surfaces during pleural photodynamic therapy</title> . , 2002, 4612, 102-113. | | 2 |
| 209 | Temperature dependence of commercially available diode detectors. Medical Physics, 2002, 29, 622-630. | 3.0 | 43 |
| 210 | In vivo light dosimetry for motexafin lutetium-mediated PDT of recurrent breast cancer. Lasers in Surgery and Medicine, 2002, 31, 305-312. | 2.1 | 65 |
| 211 | In vivo reflectance measurement of optical properties, blood oxygenation and motexafin lutetium uptake in canine large bowels, kidneys and prostates. Physics in Medicine and Biology, 2002, 47, 857-73. | 3.0 | 46 |
| 212 | Modeling the output ratio in air for megavoltage photon beams. Medical Physics, 2001, 28, 925-937. | 3.0 | 33 |
| 213 | Clinical applications for photodymanic therapy in oncology. , 2001, , . | | Ο |
| 214 | Phase II Trial of Debulking Surgery and Photodynamic Therapy for Disseminated Intraperitoneal Tumors. Annals of Surgical Oncology, 2001, 8, 65-71. | 1.5 | 104 |
| 215 | Characteristics of bremsstrahlung in electron beams. Medical Physics, 2001, 28, 1352-1358. | 3.0 | 32 |
| 216 | Phase II Trial of Debulking Surgery and Photodynamic Therapy for Disseminated Intraperitoneal Tumors. Annals of Surgical Oncology, 2001, 8, 65-71. | 1.5 | 1 |

| # | Article | IF | CITATIONS |
|-----|---|-----|-----------|
| 217 | The impact of primary tumor volume on local control for oropharyngeal squamous cell carcinoma treated with radiotherapy. , 2000, 22, 1-5. | | 59 |
| 218 | Comparison between isotropic and nonisotropic dosimetry systems during intraperitoneal photodynamic therapy. , 2000, 26, 292-301. | | 45 |
| 219 | Comparison between isotropic and nonisotropic dosimetry systems during intraperitoneal photodynamic therapy. Lasers in Surgery and Medicine, 2000, 26, 292. | 2.1 | 1 |
| 220 | Photon beam skin dose analyses for different clinical setups. Medical Physics, 1998, 25, 860-866. | 3.0 | 59 |
| 221 | The equivalent square concept for the head scatter factor based on scatter from flattening filter. Physics in Medicine and Biology, 1998, 43, 1593-1604. | 3.0 | 18 |
| 222 | A generalized solution for the calculation of in-air output factors in irregular fields. Medical Physics, 1998, 25, 1692-1701. | 3.0 | 29 |
| 223 | Electron contamination in 8 and 18 MV photon beams. Medical Physics, 1998, 25, 12-19. | 3.0 | 50 |
| 224 | An equivalent square field formula for determining head scatter factors of rectangular fields. Medical Physics, 1997, 24, 1770-1774. | 3.0 | 48 |
| 225 | Performance evaluation of a diode array for enhanced dynamic wedge dosimetry. Medical Physics, 1997, 24, 1173-1180. | 3.0 | 39 |
| 226 | Commissioning of enhanced dynamic wedge on a ROCS RTP system. Medical Dosimetry, 1997, 22, 231-236. | 0.9 | 6 |
| 227 | Concurrent platinum-based chemotherapy and hyperfractionated radiotherapy with late intensification in advanced head and neck cancer. International Journal of Radiation Oncology Biology Physics, 1997, 39, 721-729. | 0.8 | 23 |
| 228 | Tissue-phantom ratios from percentage depth doses. Medical Physics, 1996, 23, 629-634. | 3.0 | 25 |
| 229 | Phonon attenuation in glasses studied by picosecond ultrasonics. Physica B: Condensed Matter, 1996, 219-220, 296-298. | 2.7 | 18 |
| 230 | Characterizing output for dynamic wedges. Medical Physics, 1996, 23, 1213-1218. | 3.0 | 23 |
| 231 | Experimental determination of the dose kernel in high-energy x-ray beams. Medical Physics, 1996, 23, 505-511. | 3.0 | 30 |
| 232 | Electron disequilibrium in high-energy x-ray beams. Medical Physics, 1996, 23, 1867-1871. | 3.0 | 12 |
| 233 | Doses near the surface in high-energy x-ray beams. Medical Physics, 1995, 22, 465-468. | 3.0 | 36 |
| 234 | X-ray source and the output factor. Medical Physics, 1995, 22, 793-798. | 3.0 | 43 |

| # | Article | IF | CITATIONS |
|-----|---|-----|-----------|
| 235 | Scattered photons from wedges in high-energy x-ray beams. Medical Physics, 1995, 22, 1339-1342. | 3.0 | 10 |
| 236 | The fraction of photons undergoing head scatter in X-ray beams. Physics in Medicine and Biology, 1995, 40, 1127-1134. | 3.0 | 49 |
| 237 | The head-scatter factor for small field sizes. Medical Physics, 1994, 21, 65-68. | 3.0 | 67 |
| 238 | <title>CT reconstruction of x-ray source profile of a medical accelerator</title> . , 1994, , . | | 5 |
| 239 | Blocking Factors for Irregular Electron Fields. International Journal of Radiation Oncology Biology Physics, 1993, 27, 302. | 0.8 | 0 |
| 240 | Attenuation of longitudinal-acoustic phonons in amorphousSiO2at frequencies up to 440 GHz. Physical Review B, 1991, 44, 4281-4289. | 3.2 | 158 |